Anti-phosphotyrosine (1:1000, 4G10) was obtained from Millipore. Rabbit anti-PDGFR-β antibody has been described before [4]..

Generation of CCN3 mutant mice

A BAC (bacterial artificial chromosome) clone containing the *CCN3* was screened from a mouse BAC library (Research Genetics). Using the BAC, a targeting vector was constructed to delete the genomic region encompassing exons 1, 2 and a part of 3 for complete elimination of the CCN3 transcription (Figure 4A). This vector was introduced into R1 ES cells and homologous recombinants were cloned through selection with antibiotics and verification of the genotype. Chimeric mice with the targeted ES cell clones were developed to obtain mice heterozygously transmitting the CCN3-knockout genome. Their descendants were backcrossed to C57Bl/6J (The Jackson Laboratory) for at least 6 generations and maintained as heterozygotes. The heterozygous mice were inter-crossed to produce homozygous offspring. CCN3 null and wild-type male mice that were 10 weeks of age were used for the experiments. All of the experimental procedures were performed in accordance with Chiba institutional guidelines for animal research. The body weight, blood pressure, fasting blood glucose levels and HbA_1c were measured at the time of sacrifice. The blood glucose level was

measured by a Medisafe mini system (TERUMO Corporation) and the blood pressure was measured by the tail cuff method using a softron BP-98A (Softron).

Genotyping of mutant mice

Genomic southern hybridization (Supplemental Figure 2A) and PCR (Supplemental Figure 2B) using the genomic DNA extracted from ES cells and tails were used to determined the *CCN3* genotype. The sequences of the PCR primers for amplifying the CCN3-intact and CCN3-knockout genome indicated in Figure 4A are c: CTTCCTGCTCTTCCATCTCT, d: AATGCCAGTCTGGTTGTTGG, e: TGCATCTGAGCAGTTCTGAG, f: CTCGTGCTTTACGGTATCG.

PCR amplification of genomic DNA extracted from tail biopsies was used to genotype the CCN3 mutant mice. Briefly, tail samples were incubated in a lysis buffer containing 0.2M NaCl, 0.02M EDTA, 0.05M Tris HCl, 0.5% SDS and 0.5 mg/ml proteinase K overnight at 56°C. The PCR was performed using four specific oligonucleotide primers for amplifying the wild-type and knock-in alleles. A 1.4 kb band corresponds to the mutant allele, while a 381-bp band corresponds to the wild-type allele (Supplementary Figure 2A). The PCRs contained 2 μl 10 × PCR buffer with $MgCl_2$, 2 μl dNTPs (0.25 mM), 0.4 μl primers (1 mM), 0.2 μl Taq DNA polymerase (5 U/μl, ExTaq, Takera), 1 μl

DNA template and distilled H_2O in a final volume of 20 μl. Amplification was performed using an Applied Biosystem 9700 PCR machine with the following program: 94 °C for 5 min and then 94°C for 30 s, 56°C for 30 s, 72°C for 30 s for 30 cycles and finally 72°C for 2 min.

Immunohistochemistry

Mice aortas were frozen in OCT compound and then were cut into 10 μm sections. The sections were air-dried, fixed in ice-cold methanol for 10 min, rinsed in PBT (phosphate-buffered saline (PBS) with 0.1% Tween 20) and blocked in PBT containing 0.5% BSA for 30 min. Primary antibodies were diluted in 0.5% BSA in PBT and applied overnight at 4°C. After rinsing several times with PBT, fluorophore-conjugated secondary antibodies were applied for 2 hr. The sections were then rinsed in PBT, nuclear stained with Hoechst 33342 (1:200; Dojindo), mounted (Fluoromount G, SouthernBiotech) and viewed with a fluorescence microscope (Axio Oberver, Leica) or with a confocal laser scanning microscope (Leica LSM5 PASCAL). The images were processed using Adobe Photoshop. The following antibodies were used: rabbit anti-CCN3 antibody (1:100, ab10888: Abcam), anti-PECAM-1 antibody (1:200: MEC 13.3: BD pharmingen), anti-human smooth muscle cell antibody (1:100: 1A4: DAKO).

Immunocytochemistry

SMC were cultured on Lab-Tek II chamber slides (Nalge Nunc International), deprived of serum for 24 hr and stimulated either with 1 ng/ml TGF-β or 100 ng/ml CCN3 for 30 min. Next, the cells were fixed in ice-cold methanol for 10 min, rinsed with PBS and incubated in a blocking buffer of 0.5% BSA, 0.25% Tween 20 in PBS for 30 min at room temperature. The slides were then incubated with an anti ICN1 antibody (Val 1774, 1:100 dilution, Cell signaling) overnight at 4°C, washed with PBS, followed by incubation with 1:1000 dilution of fluorescent-conjugated secondary antibody (Alexa Fluor 488 goat anti rabbit IgG, Invitrogen) for 2 hr at room temperature. The slides were then washed with in PBS, nuclear stained with Hoechst 33342 and mounted with a fluorescence mounting medium.

Femoral Artery Injury

The femoral arteries of the mice were injured using a photochemically-induced thrombosis method. The mice were anesthetized with the intraperitoneal administration of pentobarbital (50 μg/g body weight). Rose-Bengal dye (10 mg/mL in phosphate-buffered saline) was then injected into the orbital venous plexus (25 μg/g

body weight). Meanwhile, the left femoral artery was carefully exposed and transilluminated with a heat-absorbing filter (Hamamatsu photonics) for 10 min. This procedure resulted in local intraluminal thrombus formation accompanied by endothelial injury [5]. Twenty-one days later, the mice were anesthetized and perfusion fixed in 2% formaldehyde in PBS.

Luciferase assay

SMC were plated in 12-well dishes at 50% confluence and transfected with 400 ng per well p3TP-lux construct that contained three consecutive TPA response elements [6] and a portion of the plasminogen activator inhibitor 1 (PAI-1) promoter region by Fugene 6 transfection reagent (Roche Molecular Biochemicals). At 6 hr-post-transfection, cells were deprived of serum for 24 hr. Thereafter, the cells were stimulated either with 1 ng/ml TGF-β or 100 ng/ml CCN3 for 16 hr. The luciferase activities in the cell lysate were measured in a 1420 ARVO SX multilabel counter (Wallac, Inc, Gaithersburg, MD) using the Dual Luciferase Reporter Assay System (Promega, Madison, WI). To correct for potential variation in transfection efficiency, 400 ng per well pRL-TK vector (Promega) was cotransfected in all experiments. All assays were performed in quadruplicate and then were repeated three times.

Induction of diabetes

Diabetes was induced in mice by intraperitoneally injecting them with streptozotocin (STZ; Sigma Chemical, St. Louis, MS, USA). STZ was dissolved in an ice-cold citrate buffer at pH 4.6 and immediately injected into the mice at a dose of 100 mg·kg body weight^{-1}·day^{-1} for 3 days. Control mice received only the citrate buffer. The first day of STZ injection was designated as day 0. On day 14, the mice were killed, and their aortas were dissected. The blood glucose levels were significantly higher in the STZ-induced diabetic mice (n = 4) than in the control mice (n = 8) (306.3 (30.9) mg/dl vs. 120.4 (30.0) mg/dl, $P < 0.01$). Moreover, the body weight of STZ-induced diabetic mice was significantly lower than that of the control mice (23.3 (1.0) g vs. 25.8 (1.0) g, $P < 0.01$). We also treated some STZ-induced diabetic mice (n = 6) with 0.1 U/body of insulin from day 5 until day 14. The blood glucose levels of insulin-treated mice were significantly lower than those of untreated insulin (234 (60.6) mg/dl vs. 306.3 (30.9) mg/dl, $P < 0.05$).

Legends to Supplemental Figures

Supplemental Figure I.

Expression of CCN3 in VSMCs and the effects of CCN3 on the VSMCs.

A. The expression of CCN3 mRNA was examined and compared with the culture time by using RT-PCR. One representative of 2 experiments is shown.

B. The effects on CCN3 on VSMC proliferation. The number of cells was counted in the absence (open bars) or presence (filled bars) of CCN3 at the indicated times.

C. Effects of CCN3 on the cell cycle of VSMCs. Flow cytometric analysis of the cell cycle distribution of VSMCs. The histograms show a representative of 3 experiments.

D. Percentage of cells in the S+G2/M phase. VSMCs were initially serum-starved for 24 h and then treated with CCN3 or TGF-β for 24 h in the presence or absence of FBS. Cell cycle distribution was determined by flow cytomeric analysis of the DNA content in propidium iodide. *$P < 0.05$, **$P < 0.001$

E. Cells were serum-starved for 24 h and then incubated with 1 ng/ml TGF-b1 or 100 ng/ml CCN3 at the indicated time points at 37°C. Thereafter, the expression of p21 and p15 was examined and compared with that of GAPDH by RT-PCR.

F. VSMCs were transiently transfected with p3TP-Lux, a TGF-b responsive luciferase reporter construct, deprived of serum for 24 h, and then stimulated either with 1 ng/ml TGF-b or 100 ng/ml CCN3 for 16 h. The luciferase activity in the cell lysates was

measured using the Dual-Luciferase Reporter Assay System. All assays were performed in quadruplicate and were then repeated 3 times.

Supplemental Figure II.

CCN3 inhibited VSMC proliferation by inhibiting the Notch signaling pathway.

(A) We examined the effects of a γ-secretase inhibitor (GSI), which blocks the Notch signaling pathway, on the inhibition of VSMC proliferation by CCN3, using BrdU incorporation as described in the legends to Figure 2. Data are presented as mean (SE); all determinations were performed in triplicate. (B) We examined the effects of RPMS-1, a known blocker of the RBP-J-mediated Notch signaling pathway, on the expression of p21 as well as Hey1 by RT-PCR as described in the legends to Figure 3A.

Supplemental Figure III.

Effects of CCN3 on PDGFR-ß expression and its tyrosine phosphorylation and ERK activation.

SMCs were seeded in 100-mm dishes and serum-starved for 24 h. The cells were then treated with 100 ng/ml CCN3 or 50 ng/ml PDGF-BB for 5 min at 37°C.

After incubation, the cells were lysed. The lysates were either directly separated by 10% SDS-PAGE followed by immunoblotting with anti-phospho ERK or anti-ERK antibody (A) or immunoprecipitated with anti-PDGFR-β antibody and separated with 5% SDS-PAGE, followed by immunoblotting with anti-phospho tyrosine (Tyr) antibody or anti-PDGFR-β antibody (B).

Supplemental Figure IV.

Generation of *CCN3*$^{-/-}$ mice.

A. Genomic Southern analysis of the recombinant ES clone. The genomic DNA of the ES clone was digested with *Eco*RI and analyzed by Southern hybridization, using genomic fragment a or b, as indicated in Figure 4A. The representative results of the original ES cells (+/+) and homologous recombinant clone (+/-) are shown.

B. PCR analyses of the targeted mouse. The genotype was determined by PCR using the specific primers indicated in Figure 4A for wild type (c and d) and targeted alleles (e and f). Representative results of a homozygote (-/-), heterozygote (+/-), and wild type (+/+). The 0.4-kb and 1.5-kb bands indicate the wild and targeted genomes, respectively.

C. RT-PCR analysis for *CCN3* mRNA in heart RNA obtained at postnatal day 28. Homozygous mice did not express a 561-bp band derived from the *CCN3* mRNA.

Supplemental Figure V.

Vascular wall responses to the injury to the femoral arteries induced by photochemically induced thrombosis (Pit).

The femoral arteries of the mice were injured using photochemically induced thrombosis. One week after Pit, BrdU (50 mg/kg) was injected into the peritoneal spaces 6 h before sacrificing the mice. The femoral arteries were excised, fixed with 4% paraformaldehyde, embedded in OCT compound, and cut into 10-μm sections. The sections were stained with anti-BrdU antibody (A) or anti-PECAM antibody and co-stained with anti-alpha smooth muscle cell actin (ASMA) antibody (B).

From each group, 3 animals ($CCN3^{-/-}$ and $CCN3^{+/+}$) were examined, which yielded essentially similar results, and the representative results are shown in this figure.

Supplemental Figure VI.

CCN3 expression in the aorta of STZ-induced diabetic mice as compared to the wild-type controls. (A) Diabetes was induced in 8-week-old male mice by

intraperitoneal injections of STZ. After 4 weeks of STZ injections, the aorta was dissected, snap-frozen in OCT, sectioned, stained using anti-CCN3-specific antibody, and compared to the non-diabetic controls (n = 3 in each group). (B) The CCN3-positive areas were measured and compared with the total area of the medial layer. At least 3 discontinuous aortic sections from each animal were used and compared statistically. *$P < 0.01$ compared with wild-type controls. (C) The STZ-induced diabetic mice were treated with 0.1 U/body of insulin from day 5 until day 28. The aorta was then dissected, snap-frozen in OCT, sectioned, stained using anti-CCN3-specific antibody, and compared with the non-diabetic control. This figure is a representative of 4 animals, with each yielding essentially similar results.

References

1. Honjo S, Yokote K, Fujimoto M, Takemoto M, Kobayashi K, Maezawa Y, Shimoyama T, Satoh S, Koshizaka M, Takada A, Irisuna H, Saito Y. Clinical outcome and mechanism of soft tissue calcification in Werner syndrome. *Rejuvenation Res.* 2008;11:809-819.
2. Smith PR, de Jesus O, Turner D, Hollyoake M, Karstegl CE, Griffin BE, Karran L, Wang Y, Hayward SD, Farrell PJ. Structure and coding content of CST (BART) family RNAs of Epstein-Barr virus. *J Virol.* 2000;74:3082-3092.
3. Deitch AD, Law H, deVere White R. A stable propidium iodide staining procedure for flow cytometry. *J Histochem Cytochem.* 1982;30:967-972.

4. Yokote K, Mori S, Hansen K, McGlade J, Pawson T, Heldin CH, Claesson-Welsh L. Direct interaction between Shc and the platelet-derived growth factor beta-receptor. *J Biol Chem.* 1994;269:15337-15343.
5. Kikuchi S, Umemura K, Kondo K, Saniabadi AR, Nakashima M. Photochemically induced endothelial injury in the mouse as a screening model for inhibitors of vascular intimal thickening. *Arterioscler Thromb Vasc Biol.* 1998;18:1069-1078.
6. Goto D, Nakajima H, Mori Y, Kurasawa K, Kitamura N, Iwamoto I. Interaction between Smad anchor for receptor activation and Smad3 is not essential for TGF-beta/Smad3-mediated signaling. *Biochem Biophys Res Commun.* 2001;281:1100-1105.

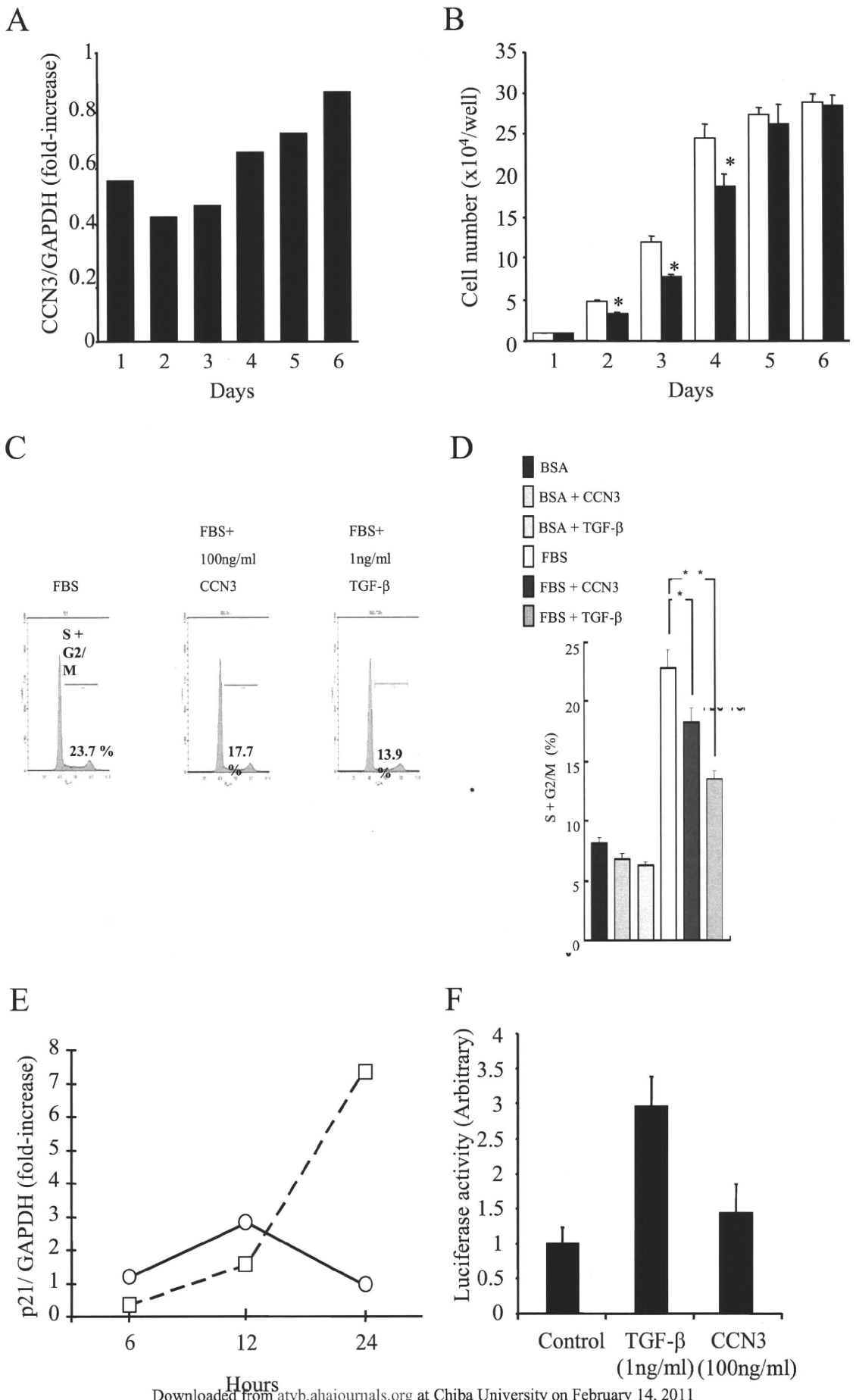

Supplementary Figure I

A

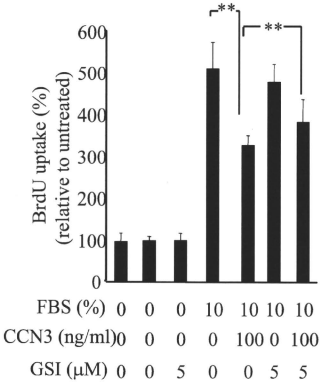

B

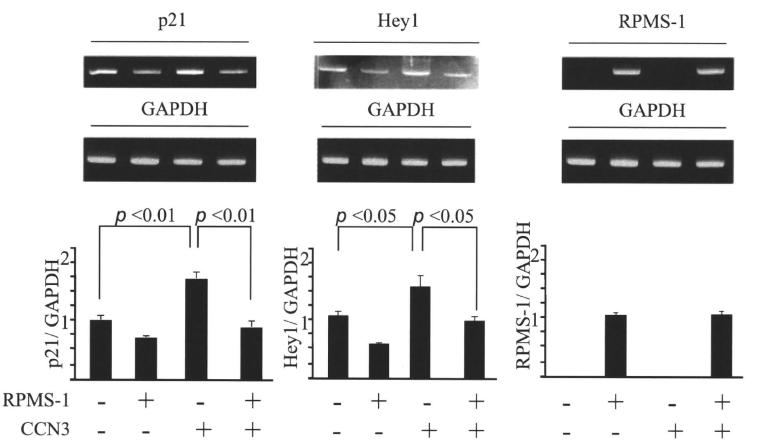

Supplementary Figure II

A

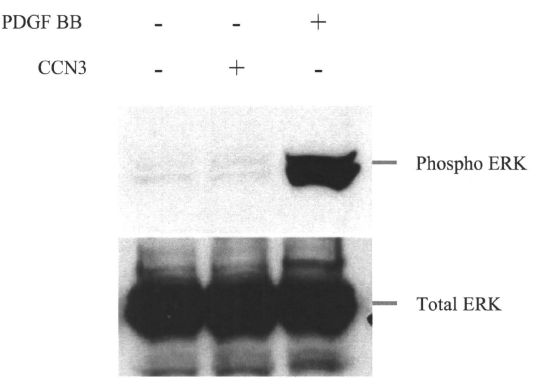

B

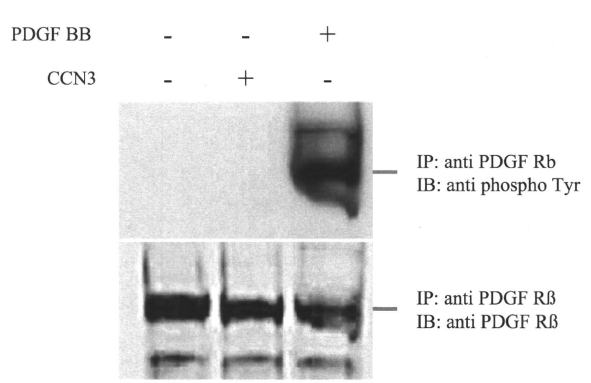

Supplementary Figure III

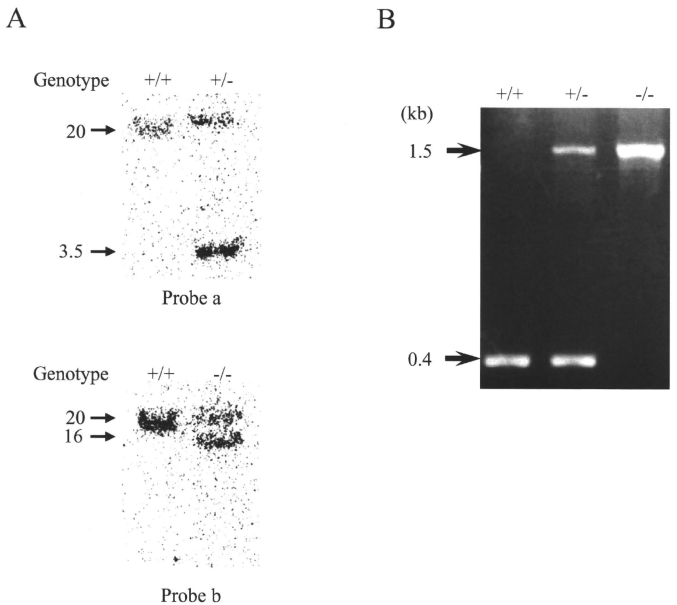

Supplementary Figure IV

A

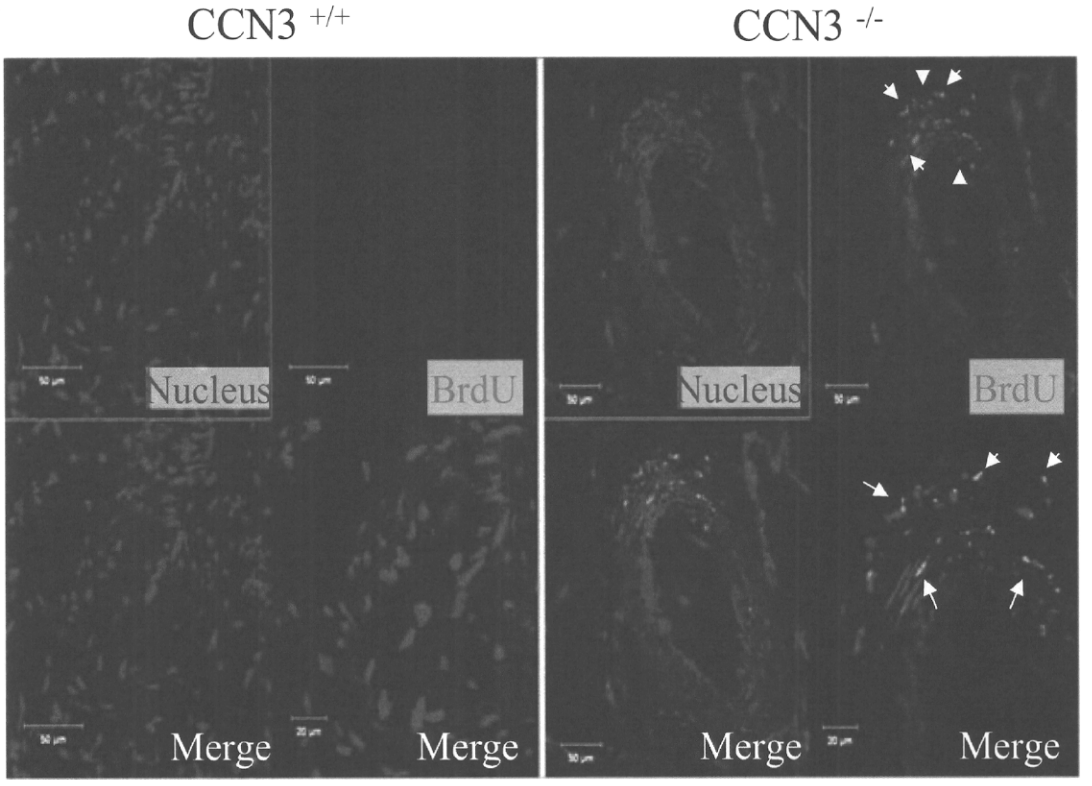

B

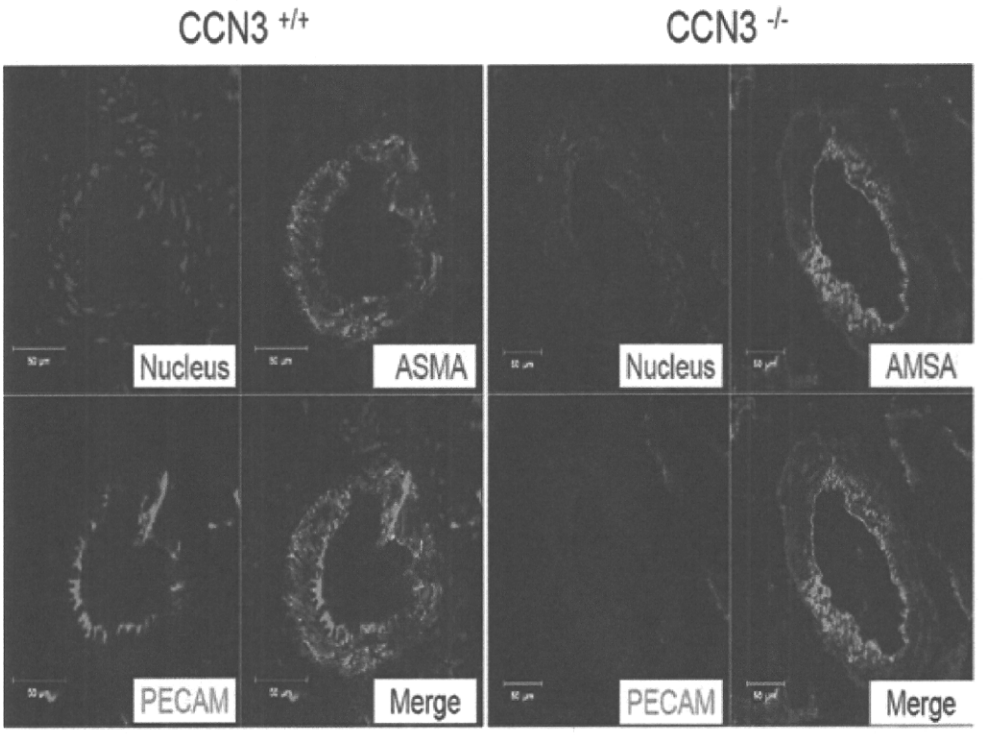

Supplementary Figure V

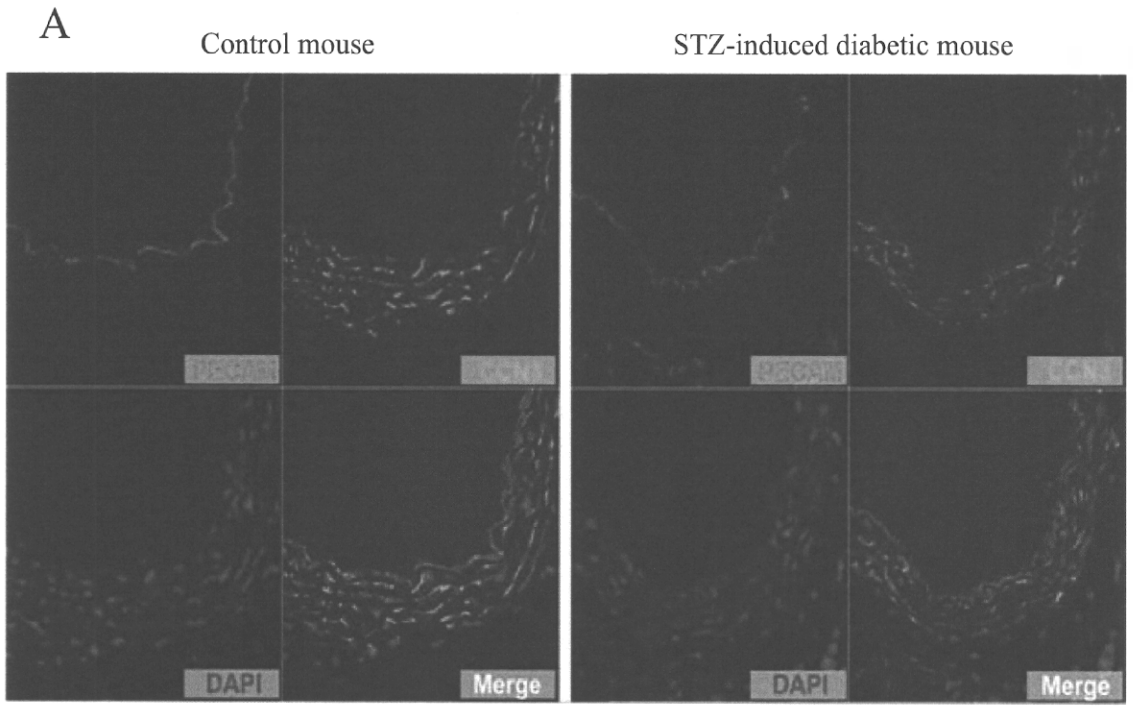

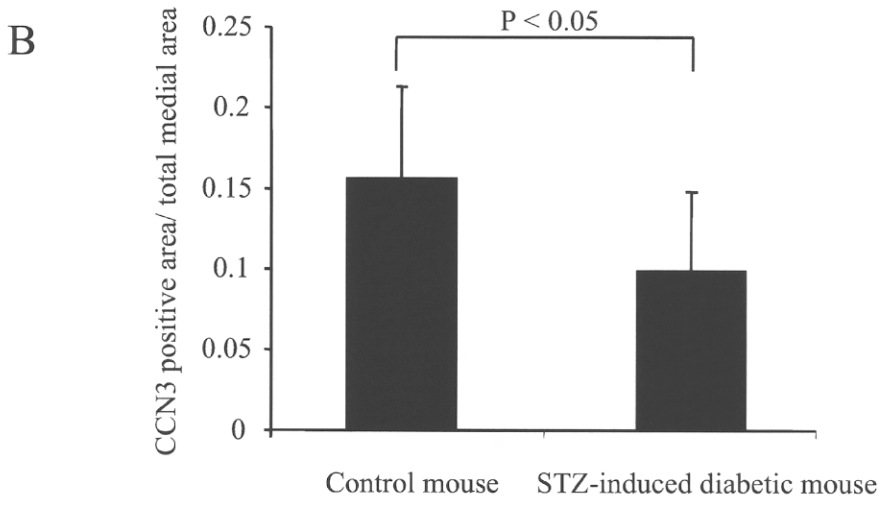

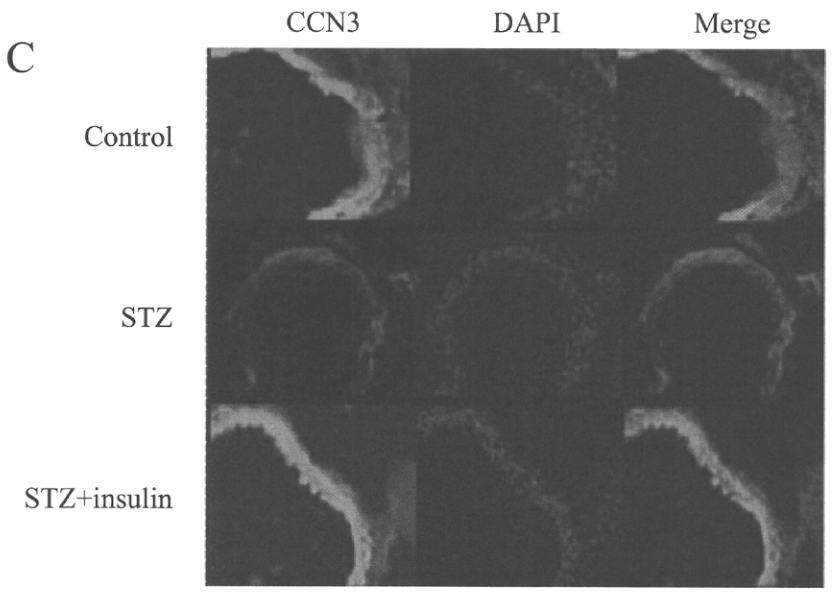

Supplementary Figure VI

Geriatrics Gerontology INTERNATIONAL 1st Impact Factor in June 2010 Medline Indexed

Geriatr Gerontol Int 2010; **10:** *319–323*

CASE REPORT

Primary lung cancer associated with Werner syndrome

Shunichiro Ohnishi,[1,2] Masaki Fujimoto,[1,2] Takashi Oide,[3] Yukio Nakatani,[3] Yuya Tsurutani,[1,2] Masaya Koshizaka,[1,2] Morito Mezawa,[1,2] Takahiro Ishikawa,[1,2] Minoru Takemoto[1,2] and Koutaro Yokote[1,2]

Departments of [1]Clinical Cell Biology and Medicine, and [3]Diagnostic Pathology, Chiba University Graduate School of Medicine, and [2]Department of Medicine, Division of Diabetes and Endocrinology, Chiba University Hospital, Chiba, Japan

A 52-year-old man with Werner Syndrome (WS) was admitted to our hospital for the treatment of skin ulcers on his thighs. Routine chest radiography revealed an abnormal shadow in the left upper lung field. Computed tomography (CT) revealed a poorly demarcated homogeneous mass (diameter, 4 cm) in the S1 + 2 lung area; no pleural effusion was observed. CT-guided percutaneous needle biopsy revealed the presence of an adenocarcinoma. Other imaging studies did not reveal any lymph-node involvement or presence of metastatic lesions. The patient was diagnosed with stage IB adenocarcinoma (T2N0M0), and a left upper lobectomy was successfully carried out; postoperative wound healing was steady and uneventful, with no obvious ulcer formation. Primary lung cancers very rarely develop in patients with WS; non-epithelial tumors are usually observed in such patients. Patients with WS usually develop severe skin problems, such as refractory skin ulcers in the extremities; however, our patient did not develop any skin-related complications after surgery. As the expected lifespan of patients with WS is increasing, we need to pay attention not only to the rare non-epithelial malignancy, but also cancer. Further, the expected short lifespan of patients with WS, as well as the possibility of skin-related problems after surgery, should not be considered while deciding whether to take the option of surgery in the case of malignancy. **Geriatr Gerontol Int 2010; 10: 319–323.**

Keywords: adenocarcinoma, progeria, skin ulcer, Werner syndrome, wound healing.

Introduction

Werner syndrome (WS), which is also called adult progeria, is an autosomal recessive disorder caused by a mutation in the gene encoding the WS protein (WRN), which is a deoxyribonucleic acid (DNA) helicase.[1] Most of the reported cases of WS are from Japan (845 of the 1200 cases that have been reported worldwide).[2] This disease is characterized by early aging phenotypes, including graying and loss of hair, juvenile cataracts, skin ulcers, insulin-resistant diabetes and neoplasms.[3,4] The major causes of death in patients with WS are malignant tumors and atherosclerotic vascular diseases, such as coronary heart disease and cerebral vascular diseases. The ratio of incidence of malignant epithelial to malignant non-epithelial tumors in patients with WS is approximately 1:1 instead of the 10:1 ratio observed in the general population.[4] In total, 8% of patients with WS develop malignant tumors, which are usually diagnosed in the second or third decade of life. In this case, primary lung cancer was incidentally identified in a 52-year-old patient with WS; it was successfully treated with surgery, without any complications.

Accepted for publication 25 May 2010.

Correspondence: Assistant Professor Masaki Fujimoto MD PhD, Department of Clinical Cell Biology and Medicine, Chiba University Graduate School of Medicine, 1-8-1 Inohana, Chuo-ku, Chiba 260-8670, Japan. Email: mfujimoto@faculty.chiba-u.jp

Case report

A 52-year-old Japanese man was admitted to Chiba University Hospital, Chiba, Japan, for the treatment of skin ulcers on both thighs. He had been diagnosed with WS at the age of 33 years, when he had developed

doi: 10.1111/j.1447-0594.2010.00638.x

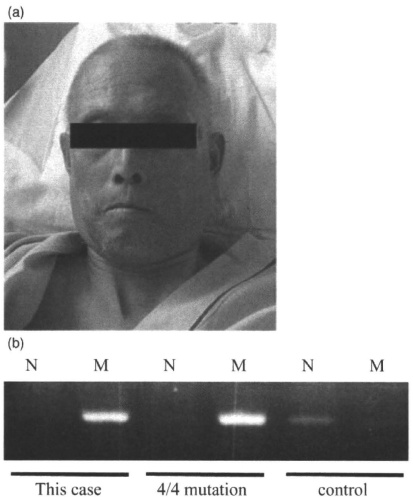

Figure 1 (a) Patient's "bird-like face", a characteristic of Werner syndrome. (b) Mutant allele-specific amplification (MASA). MASA analysis showed that the patient had the 4/4 mutation in the WRN helicase gene. M, mutation; N, normal.

bilateral cataracts. All three of his siblings had also been diagnosed with WS; however, no parental consanguinity had been reported. He had developed premature graying at the age of 15 years and was diagnosed with insulin-resistant diabetes and dyslipidemia at the age of 35 years. Since the age of 48 years, he had been treated with 10 mg of atrovastatin and 15 mg of pioglitazone. He had smoked 20 cigarettes/day from 20 to 40 years-of-age. Both his lower legs were amputated at the age of 51 years, because of intractable skin ulcers and osteomyelitis. On physical examination, we observed that he had facial features characteristic of WS; that is, he had a "bird-like" face (Fig. 1a). His voice was high pitched and hoarse; this is also a characteristic feature of WS. Multiple ulcerations, and cutaneous and subcutaneous atrophy were observed in the skin.

The complete blood cell count showed mild anemia. The results of blood biochemistry were unremarkable, except for the slightly elevated fasting blood glucose level, elevated triglyceride level and decreased high-density lipoprotein cholesterol level. To confirm the diagnosis of WS, we carried out mutation analysis based on the mutant allele-specific amplification (MASA) method.[2] The DNA from the peripheral blood leukocytes showed marked amplification for the genomic sequence corresponding to mutation 4/4 in WRN helicase, whereas this amplification was not seen in the case of control DNA (Fig. 1b); thus, the diagnosis of WS was confirmed by genetic analysis.

The patient underwent routine chest radiography on admission, which showed an abnormal shadow in the left upper lung field (Fig. 2a). CT of the lung revealed a homogeneous and poorly demarcated mass (diameter, 4 cm) in the S1 + 2 lung area; no calcification was observed (Fig. 2b). Although a portion of the pleura was invaded by the tumor, no pleural effusion was detected. The hilar, mediastinal and axillary lymph nodes were not enlarged. The levels of tumor markers for lung cancer including CEA, pro GRP, SLX and CYFRA were all within the normal range. CT-guided needle biopsy revealed the presence of an adenocarcinoma.

Magnetic resonance imaging (MRI) of the head, and CT scan and ultrasonography of the abdomen did not show any metastatic lesions. Bone scintigraphy only showed old rib fractures. The left upper lung lesion was histopathologically diagnosed as pulmonary adenocarcinoma and clinically staged as stage 1B (cT2N0M0). After providing informed consent, the patient underwent left upper lobectomy with mediastinal lymph node dissection. During the surgery, pleural indentation without pleural effusion was observed (Fig. 2c). The procedure was successful, and there were no complications.

The resected left upper lobe of the lung contained a subpleural tumor (2.8 × 2.4 × 2.2 cm), which contained solid white nodules. Although the tumor had extensively invaded the adjacent pleurae, the invasion did not extend beyond the pleurae. In addition, no metastatic lesions were observed in the lymph nodes or other lung tissue; therefore, the surgical staging of the cancer was the same as that determined before the surgery – stage IB (sT2N0M0). Histopathological examination revealed mixed cellular patterns; that is, both papillary and solid (Fig. 2d). These findings correspond to those of adenocarcinoma mixed subtype, with lymphocytic and plasma cell infiltration. No pleural invasion was observed. Pathological staging was stage IA (pT1, pN0, pm, n0, p0, br-).

Postoperative wound healing was steady and uneventful, with no obvious ulcer formation or infection. The patient was discharged on the 90th hospital day.

Discussion

Here, we report the case of a patient with WS who developed primary lung cancer that was successfully resected. WS patients usually die in the fourth decade of life, because of premature atherosclerosis and/or malignant neoplasms.[5] Strangely, in patients with WS, the incidence of malignancies of mesenchymal origin (sarcoma) was higher than that of the cancer.[3] The mechanism underlying the development of neoplasms in patients with WS remains unclear. However, several